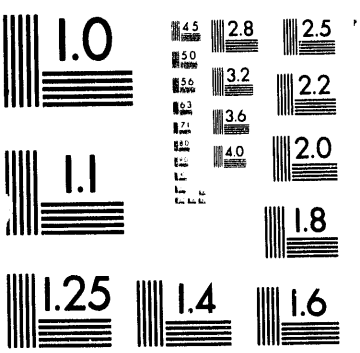
1.0
1.1
1.25
1.4
1.6
1.8
2.0
2.2
2.5
2.8
3.2
3.6
4.0
4.5
5.0
5.6
6.3
7.1
8.0
9.0

1 of 1

# MECHANICAL PROPERTIES OF NANOPHASE MATERIALS*

Richard W. Siegel
*Materials Science Division*
*Argonne National Laboratory, Argonne, IL 60439*

Gretchen E. Fougere
*Department of Materials Science and Engineering*
*Northwestern University, Evanston, IL 60208*

November 1993



**INVITED TUTORIAL LECTURE** presented at the NATO Advanced Study Institute on Nanophase Materials: Synthesis-Properties-Applications, Corfu, Greece, June 20-July 2, 1993; to be published in Nanophase Materials: Synthesis-Properties-Applications, G. C. Hadjipanayis and R. W. Siegel, eds. (Kluwer, Dordrecht, 1994), in press.

*Work supported by the U.S. Department of Energy, Basic Energy Sciences-Materials Sciences, under Contract #W-31-109-ENG-38 at Argonne National Laboratory and Grant DE-FG02-86ER45229 at Northwestern University.

# MECHANICAL PROPERTIES OF NANOPHASE MATERIALS

RICHARD W. SIEGEL
*Materials Science Division*
*Argonne National Laboratory*
*Argonne, Illinois 60439 USA*

GRETCHEN E. FOUGERE
*Department of Materials Science and Engineering*
*Northwestern University*
*Evanston, Illinois 60208 USA*

ABSTRACT. It has become possible in recent years to synthesize new materials under controlled conditions with constituent structures on a nanometer size scale (below 100 nm). These novel nanophase materials have grain-size dependent mechanical properties that are significantly different than those of their coarser-grained counterparts. For example, nanophase metals are much stronger and apparently less ductile than conventional metals, while nanophase ceramics are more ductile and more easily formed than conventional ceramics. The observed mechanical property changes are related to grain size limitations and/or the large percentage of atoms in grain boundary environments; they can also be affected by such features as flaw populations, strains and impurity levels that can result from differing synthesis and processing methods. An overview of what is presently known about the mechanical properties of nanophase materials, including both metals and ceramics, is presented. Some possible atomic mechanisms responsible for the observed behavior in these materials are considered in light of their unique structures.

## 1. Introduction

The mechanical properties of materials depend fundamentally upon the nature of bonding among their constituent atoms and upon their microstructures on a variety of length scales. Mechanical deformation can be either elastic (reversible) or plastic (irreversible). Elastic deformation is effected through reversible changes in the interatomic spacings or the bending and stretching of bonds between atoms; it is governed by the elastic constants or moduli of a material, which indicate how easily such deformation occurs. For metals, such deformation is in general relatively easy owing to the non-local nature of metallic bonding, but for materials with strong covalent bonding it is much more difficult.

In order to deform a material plastically, however, atomic ensembles must be displaced with respect to one another in a cooperative fashion. The easier that this process can be accomplished, the greater the ductility of the material. This deformation most frequently entails the motion of dislocations, the crystal lattice defects that facilitate such cooperative motion by localizing it and propagating this motion by a sequential disturbance of a much smaller subset of the atoms to be displaced. The unit displacement associated with a dislocation is defined by its Burgers vector, which has a magnitude that is usually on the order of an interatomic spacing and a direction that can vary between being parallel to the dislocation line (screw dislocation) or perpendicular to it (edge dislocation). Dislocation motion can be conservative ("glide") or non-conservative ("climb"); the former occurs without the creation or annihilation of atomic defects, such as vacancies, whereas the latter requires such defects and is thus a process that requires significant thermal activation.

The ease of dislocation motion and creation at dislocation sources depends upon the nature of the atomic bonding in the material and also upon the material's microstructure. It is much easier (i.e., energetically favorable) to create and move dislocations, both of which involve bond bending and breaking, in metallically bonded materials than in either ionic or covalent solids. In ionic materials, charge neutrality conditions provide stringent constraints on the motion of such extended defects, while in strongly covalent solids, the breaking and bending of these highly directional bonds can require a great deal of energy. Even for metallic systems, where the degree of covalency can vary from essentially zero in a simple metal to moderate in a refractory transition metal to rather strong in an intermetallic compound, the difficulty in creating and moving dislocations can vary significantly, leading to very different mechanical behavior.

In some cases, plastic deformation can also occur by other mechanisms which depend more strongly on time and temperature than dislocation glide. Such deformation is usually called "creep" and may be effected by dislocation climb, atomic diffusion, and/or such a mechanism as grain boundary sliding, in which the grains of a polycrystal slide over one another, but they remain fully bonded through the action of local diffusional healing processes in the interfaces between the grains. Creep rates in polycrystals depend strongly upon the grain size (d) and vary from inverse $d^2$ behavior in cases where the mechanism is volume diffusion controlled (Nabarro-Herring creep) to inverse $d^3$ behavior in cases in which the mechanism is interface diffusion controlled (Coble creep or Ashby-Verrall creep). Thus, as one enters the nanophase regime from conventional grain sizes and d is reduced greatly, the mechanical behavior can change dramatically.

In conventional metallic materials, strengthening during plastic deformation occurs with an increase in the dislocation density by dislocation multiplication mechanisms and the interaction between dislocations. A dislocation moves under the influence of a stress applied to the material; upon encountering an obstacle in its path, this stress must be increased to continue its motion. Obstacles to dislocation motion may be the stress fields of other dislocations or alloying elements, precipitates, or grain boundaries. It is thus common to strengthen these materials (when desired) by a variety of methods to make dislocation motion more difficult. These include decorating them with impurities ("solute strengthening") that would have to be dragged along by the moving dislocation (or broken away from) or introducing obstacles to their motion, such as precipitates ("obstacle strengthening") or other dislocations ("work hardening"), in their paths.

Grain size reduction (refinement) in polycrystals can also yield improvements in mechanical properties, such as strength and hardness, through the introduction of additional grain boundaries that can act as effective barriers to dislocation motion. Hence, it is predicted that grain size refinement from the conventional tens to hundreds of microns to the nanophase regime below 100 nm should lead to improvements in these mechanical properties. However, grain size refinement may also have negative impacts on other mechanical properties, such as creep rate and ductility. On the other hand, in materials that are conventionally quite strong but very brittle, such as ceramics and intermetallic compounds, enhanced ductility from grain size reduction can potentially offer tremendous processing and performance advantages.

How these various mechanisms that control the mechanical behavior of materials change as one enters the nanophase grain size regime is of great current interest and the subject of this tutorial review in our NATO Advanced Study Institute on nanophase materials. Even though a number of mechanical property changes can be expected with decreasing grain size, the extent to which these properties are altered can be significantly affected in this grain size regime, since traditional deformation mechanisms might not be operative at all or to the same degree and new mechanisms could arise. A detailed introduction to mechanical behavior in conventional materials and how it changes as grain sizes are decreased is well beyond the scope of this review. However, an earlier NATO-ASI on the mechanical properties and deformation behavior of materials having ultrafine microstructures was held in 1992; its Proceedings [1] can be usefully consulted to provide a much broader and more detailed background than can be realistically made available here. Also, some basic treatises [2, 3] on the deformation mechanisms and mechanical behavior of conventional materials may be useful background reading.

## 2. Structures of Nanophase Materials

The structures of nanophase materials on a variety of length scales have an important bearing on their mechanical properties. They are dominated by ultrafine grain sizes and the large number of associated interfaces. In addition, however, other structural features such as pores (and larger flaws), grain boundary junctions, and other crystal lattice defects that can depend upon the the manner in which these materials are synthesized and processed play a significant role. It has become increasingly clear that all of these structural aspects of nanophase materials must be considered in trying to fully understand the mechanical behavior of these new materials.

### 2.1. GRAINS

Our present knowledge of the grain structures of nanophase materials, whether formed by cluster consolidation, intense mechanical deformation, or crystallization from amorphous precursors, has resulted primarily from direct observations using transmission electron microscopy (TEM) [4-7]. A typical high resolution image of a nanophase Pd sample formed by the consolidation of gas-condensed clusters is shown in Fig. 1. TEM has shown that the grains in such nanophase compacts are essentially equiaxed, similar to the atom clusters from which they were formed, although departures from spherical structures

are expected simply from the efficient packing of the clusters during consolidation. The grains also appear to retain the narrow (ca. + 25 % FWHM) log-normal size distributions typical of the clusters formed in the gas-condensation method, since measurements of these distributions before or after cluster consolidation by dark-field electron microscopy yield similar results. Grain size distributions in deformation or crystallization produced nanostructructures can be somewhat broader, but the grains are similarly equiaxed.

The observations (e.g., [8]) that the densities of nanophase materials consolidated from equiaxed clusters extend well beyond the theoretical limit (78%) for the densest packing of undeformed identical spheres indicate that an extrusion-like deformation of the clusters must result during the consolidation process, filling (at least partially) the pores among the grains. Such observations indicate that cluster extrusion in forming nanophase grains may result from a combination of deformation and diffusion processes. These processes are also evident from recent scanning tunneling microscopy observations [9] on nanophase Pd and Ag. An example from Ag is shown in Fig. 2.

Observations by both electron and x-ray scattering indicate, however, that no apparent preferred crystallographic orientations or "texture" of the grains results from their uniaxial consolidation and that the grains in the nanophase compact are essentially randomly oriented with respect to one another. This is interesting with respect to the fact that such deformation and annealing textures commonly observed in conventional grain size materials are the result of dislocation glide processes, which seem to be suppressed in nanophase materials, as will be discussed in the following. Indeed, only very few dislocations are observed within the grains in these ultrafine-grained materials, and these are normally in immobile or "locked" (i.e., sessile) configurations.

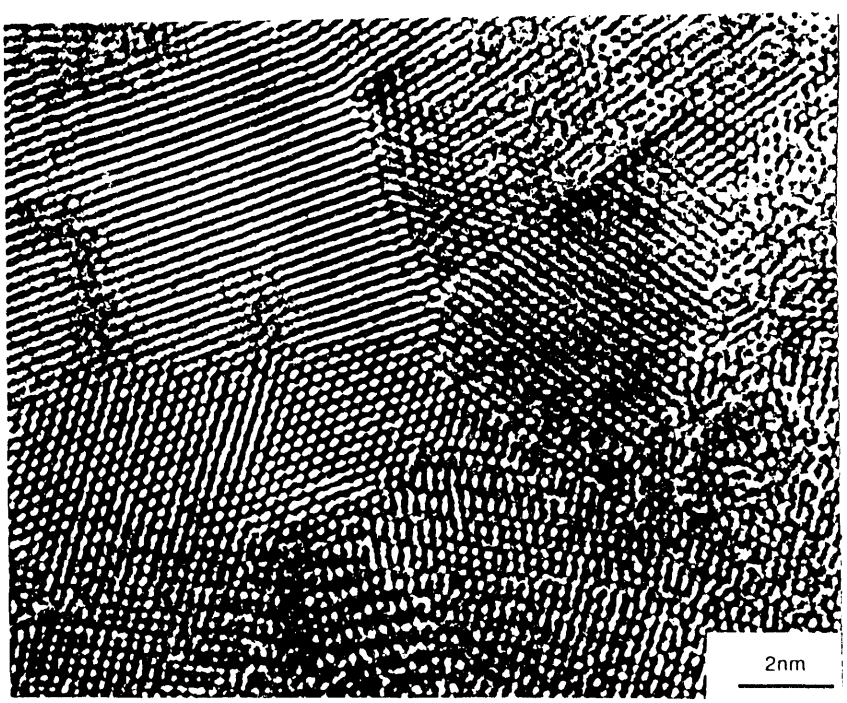


**Figure 1.** High resolution transmission electron micrograph of a typical area in cluster consolidated nanophase palladium [6].

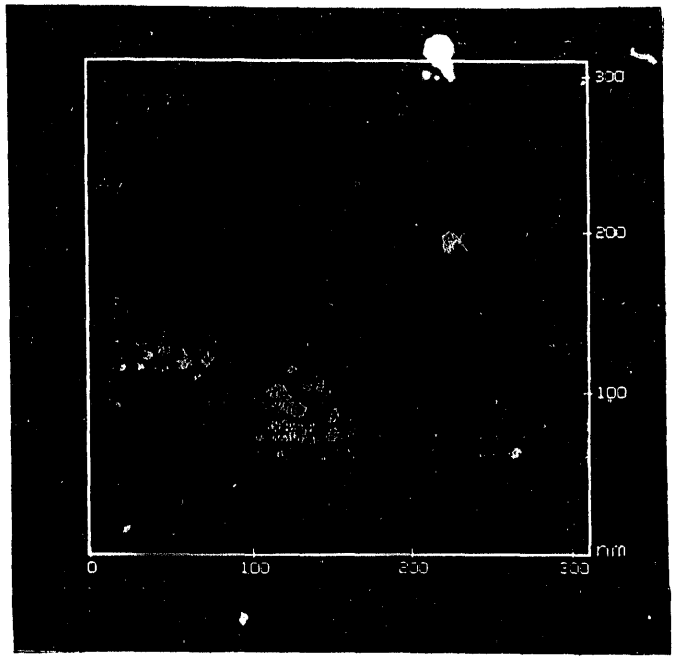


**Figure 2.** Scanning tunneling micrograph of nanophase silver [9].

2.2. PORES

All of the nanophase materials consolidated to date from clusters at room temperature have invariably posessed some porosity. This porosity has ranged from about 15-25% for ceramics to less than 5% for metals. Significant porosity can also result from the deformation or crystallization synthesis of nanophase materials. Evidence for porosity has been obtained by positron annihilation spectroscopy (PAS) [4, 10, 11], precise densitometry [8] and porosimetry [12, 13] measurements, and small angle neutron scattering (SANS) [13, 14].

PAS is primarily sensitive to small pores, ranging from single vacant lattice sites to larger voids, but PAS can probe these structures enclosed in the bulk of the material. Porosimetry measurements using the BET (Brunauer-Emmett-Teller) $N_2$ adsorption method, on the other hand, probe only pore structures open to the free surface of the sample, but BET can yield pore size distributions (although with some questions regarding their validity at nanometer pore sizes), which are unavailable from PAS. Densitometry using an Archimedes method integrates over all structures in the sample, including grains, pores (open or closed), and density decrements at defect sites as well. SANS is quite sensitive to pores in the 1-100 nm size range, but deconvolution of the scattering data can be difficult when a broad spectrum of scattering centers is present, as is often the case in nanophase materials. However, even in such a case, it has been possible recently [14] to analyze SANS data from cluster-consolidated Pd in terms of a population of small (ca. 1 nm diameter) voids presumed to be located at grain boundary intersections (triple junctions) and grain-sized voids; however, the possible scattering from grain boundaries or larger flaws was not taken into account in the analysis.

A variety of such measurements to date have shown that the porosity in nanophase metals and ceramics is primarily smaller than or equal to the grain size of the material (although some larger porous flaws have been observed by optical and scanning electron microscopy). The porosity is frequently associated with the grain boundary junctions (triple junctions) and, especially, but not only in ceramics, it is interconnected and intersects with the specimen surfaces. Fortunately, consolidation at elevated temperatures should be able to uniformly remove this porosity without sacrificing the ultrafine grain sizes in these materials. Some evidence for this has already been obtained by means of the sinter forging of nanophase ceramics [15].

It should be noted here that atomic diffusion in nanophase materials, which can have a significant bearing on their mechanical properties, such as creep and its extremely useful manifestation in superplasticity, has been found to be greatly enhanced compared with conventional materials. Measurements of self-diffusion and solute-diffusion [16-20] in as-consolidated nanophase metals (Cu, Pd) and ceramics ($TiO_2$) indicate that atomic transport can be orders of magnitude faster in these materials than in coarser-grained polycrystalline samples. However, this very rapid diffusion appears to be intrinsically coupled with the porous nature of the interfaces in these materials, since the diffusion can be suppressed back to conventional values by sintering samples to full density, as shown by measurements of Hf diffusion in $TiO_2$ before and after densification by sintering [16]. Thus, in fully densified nanophase materials, it is likely that only normal grain boundary diffusion, intensified by the large number density of available grain boundaries, will play a role in their mechanical behavior.

### 2.3. DISLOCATIONS

Dislocations are most often the lattice defect responsibile for the permanent or plastic deformation in metals and nonmetal crystalline materials. As a dislocation moves through the crystal lattice under the influence of an externally applied stress, its motion imparts a permanent microscopic displacement that taken together with the motion of other dislocations can lead to a macroscopic shape change in the sample. Dislocations may glide conservatively along specified glide or slip planes in a lattice in which the atoms are very closely packed; the energy required (Peierls energy) to move the dislocation across this atomically corrugated plane is rather minimal (generally well below ca. 0.1 eV and varying with the nature of the atomic bonding). With increased temperatures, dislocations may alternatively undergo climb by moving nonconservatively out of their glide plane by means of the creation or annihilation of atomic defects, such as vacancies, which requires expending greater energy (ca. 1 eV and varying with the bonding).

The presently available experimental evidence suggests that dislocations are seldom present [6, 21, 22, 23] in nanophase materials. When they are observed, it is primarily in those materials at the upper end of the grain size range [24] or in limited instances [7, 25] most often in immobile or locked configurations. The reason for this substantial lack of dislocations is that image forces exist in finite atomic ensembles that tend to pull mobile dislocations out of the grains, especially when they are small, in analogy with the forces on a point electrical charge near a free surface of a conducting body. This dearth of mobile dislocations will therefore mitigate their contribution to the development of plasticity unless new mobile dislocations can be readily created. Dislocations can be

created or can multiply from a variety of sources. A simple but representative example is the Frank-Read dislocation source, shown in Fig. 3, in which a dislocation line, pinned between two pinning points that prevent its forward motion on a slip plane, can bow out between these pinning points to form a new dislocation, if the stress acting on the pinned dislocation is sufficient. The critical stress to operate such a Frank-Read source is inversely proportional to the distance between the pinning points and hence will also be limited by the grain size, which limits the maximum distance between such pinning points. This suggests that dislocation multiplication in nanophase metals will become increasingly difficult as the grain size decreases. The critical stress will eventually, at sufficiently small grain sizes, become larger than the yield stress (at which plastic deformation begins) in the conventional material and could even approach the theoretical yield strength of a perfect (dislocation free) single crystal.

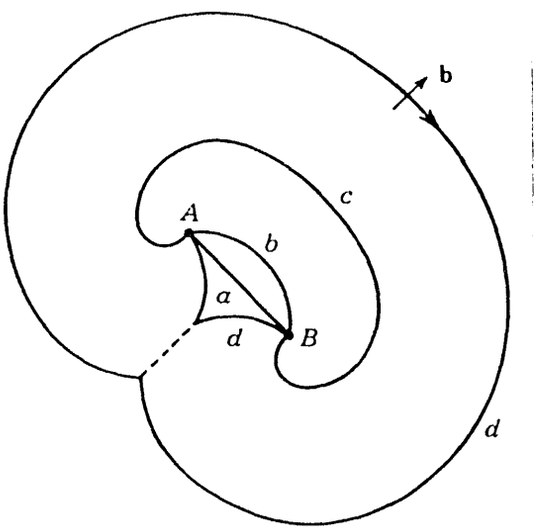


**Figure 3.** Schematic representation of a Frank-Read dislocation source. A segment of dislocation loop (a) of length L and Burgers vector **b** is pinned between points A and B in a material of shear modulus G. When the stress applied to the dislocation line segment exceeds a critical stress, $\sigma_{crit}$ = kGb/L, the dislocation bows out ($a \rightarrow b \rightarrow c \rightarrow d$) until it creates a new dislocation loop. The constant of proportionality, k, is 0.5 for an edge dislocation and 1.5 for a screw dislocation.

## 2.4. GRAIN BOUNDARIES

Owing to their ultrafine grain sizes, nanophase materials have a significant fraction of their atoms in grain boundary environments, where they occupy positions relaxed from their normal lattice sites. For conventional high-angle grain boundaries, these relaxations extend over about two atom planes on either side of the boundary, with the greatest relaxation existing in the first plane [26]. For an average grain diameter range between 5 and 10 nm, where much of the research on nanophase materials has focused, grain boundary atom percentages range between about 15 and 50%. Since such a large fraction

of their atoms reside in grain boundaries, these interface structures can play a significant role in affecting the mechanical properties of nanophase materials.

Several early investigations of nanocrystalline metals, including x-ray diffraction [27], Mössbauer spectroscopy [28], positron lifetime studies [10, 11], and extended x-ray absorption fine structure (EXAFS) measurements [29, 30], were interpreted in terms of grain boundary atomic structures that may be random, rather than possessing either the short-range or long-range order normally found in the grain boundaries of conventional coarser-grained polycrystalline materials. This randomness was variously associated [31] with either the local structure of individual boundaries (as seen by a local probe such as EXAFS or Mössbauer spectroscopy) or the structural coordination among boundaries (as might be seen by x-ray diffraction). However, direct observations by high resolution electron microscopy (HREM) [5, 6] have indicated that their structures are rather similar to those of conventional high-angle grain boundaries. An extensive review of these results has appeared elsewhere [32].

The direct imaging of grain boundaries with HREM can avoid the complications that may arise from porosity and other defects in the interpretation of data from less direct methods, such as x-ray scattering and Mössbauer spectroscopy. A HREM study [5, 6], which included both experimental observations and complementary image simulations, indicated no manifestations of grain boundary structures with random displacements of the type or extent suggested by earlier x-ray studies on nanophase Fe, Pd, and Cu [27, 29, 30]. Contrast features at the observed grain boundaries that might be associated with disorder did not appear wider than 0.4 nm, indicating that any significant structural disorder which may be present essentially extends no further than the planes immediately adjacent to the boundary plane. Such localized lattice relaxation features are typical of the conventional high-angle grain boundary structures found in coarse-grained metals. HREM investigations of grain boundaries in nanophase Cu [33] and Fe alloys [34] produced by surface wear and high-energy ball milling, respectively, appear to support this view. Recently, nuclear magnetic resonance (NMR) studies of cluster-consolidated nanophase Ag [35] have indicated that the grain boundaries in this material have an electronic structure consistent with that for conventional high-angle boundaries. However, there are indications [36, 37] that metastable grain boundary configurations do exist in some cases that can be transformed by low temperature annealing to more stable states. Whether this behavior is associated with the intrinsic grain boundary structure itself or with extrinsic grain boundary dislocation configurations and/or strains remaining from synthesis or processing remains to be clarified.

Indeed, as shown in Fig. 1 and in similar electron micrographs, the nanophase grain boundaries appear to be essentially low energy configurations exhibiting flat facets interspersed with steps. Such structures could only arise if sufficient local atomic motion occurred during the cluster consolidation process to allow the system to reach at least a local energy minimum. These observations suggest at least two conclusions [38]: first, that the atoms that constitute the grain boundary volume in cluster-assembled nanophase materials have sufficient mobility during cluster consolidation to accommodate themselves into relatively low energy grain boundary configurations; and second, that the local driving forces for grain growth are relatively small, despite the large amount of energy stored in the many grain boundaries in these materials.

## 2.5. STABILITY

The experimental observations of narrow grain size distributions, essentially equiaxed grain morphologies, and low energy grain boundary structures in nanophase materials suggest that the inherent resistance to grain growth observed for cluster-assembled nanophase materials results primarily from a sort of frustration [39]. It appears that the narrow grain size distributions normally observed in these nanophase materials coupled with their relatively flat grain boundary configurations (and also enhanced by their multiplicity of grain boundary junctions) place these ultrafine-grained structures in a local minimum in energy from which they are not easily extricated. There are normally no really large grains to grow at the expense of small ones through an Otswald ripening process, and the grain boundaries, being essentially flat, have no local curvature to tell them in which direction to migrate. Their stability thus appears to be analogous to that of a variety of closed-cell foam structures with narrow cell size distributions, which are deeply metastable despite their large stored surface energy. Such a picture now appears to have some theoretical support [40].

It should be pointed out that exceptions to this frustrated grain growth behavior would be expected if considerably broader grain size distributions were accidentally present in a sample, which would allow a few larger grains to grow at the expense of smaller ones, or if significant grain boundary contamination were present, allowing enhanced stabilization of the small grain sizes to further elevated temperatures. Occasional observations of each of these types of behavior have been made. One could, of course, intentionally stabilize against grain growth by appropriate doping by insoluble elements or composite formation in the grain boundaries. For cluster-assembled materials, such stabilization should be especially easy, since the grain boundaries are available as cluster surfaces prior to consolidation. The ability to retain the ultrafine grain sizes of nanophase materials is important when one considers the fact that it is their grain size and large number of grain boundaries that determine to a large extent their special mechanical properties.

## 2.6. STRAINS

Strains are a matter of fact in nanophase materials. Simply owing to the large number of grain boundaries, and the concomitant short distances between them, the intrinsic strains associated with such interfaces [26, 41] are always present in these nanostructured materials. Beyond these intrinsic strains, there may also be present extrinsic strains associated with the particular synthesis method. For example, intense plastic deformation synthesis of nanophase materials may lead to additional residual strains [42] that can be subsequently relieved via low temperature annealing, leaving only those intrinsic strains due to the presence of the high angle grain boundaries. Evidence for the strains in nanophase materials is now becoming available. X-ray line broadening investigations of both cluster-consolidated [8] and ball-mill attrited metallic nanophase samples [43] have indicated residual strains of about 0.1-1%, which are consistent in magnitude with the strains expected from conventional high angle grain boundaries [26] in the grain size ranges investigated. Also, NMR measurements [44] on cluster-consolidated nanophase Cu have recently yielded strain values in this range.

## 3. Mechanical Behavior

### 3.1. HARDNESS

3.1.1. *Background.* The extent to which the surface of a material deforms under stress is an indication of its hardness. Hardness, like strength, typically derives from the difficulty in creating dislocations and the impedance of their motion by the development of barriers. It is commonly measured using a Vickers microhardness tester in which a pyramidal diamond indenter with a square cross-section is loaded with a specified force and applied to the sample surface for a given period of time. It has long been observed experimentally in conventional metallic materials [45] that the hardness varies with the grain size through the empirical Hall-Petch relation:

$$H_V = \sigma_y + k_y d^{-1/2}$$

where $H_V$ is the hardness, $\sigma_y$ is the intrinsic stress resisting dislocation motion, d is the grain diameter, and $k_y$ is a constant. Many theories have been proposed to explain this hardness variation in terms of dislocations and other microstructural features. Hardness can arise from a variety of impediments to dislocation motion [3]: dislocation cells, fine particles and dispersions, grain boundaries, strain regions, point defects or solute atoms.

The original Hall-Petch [45] model treated grain boundaries as barriers to dislocation motion and was derived for large-grained materials with high dislocation densities. The Cottrell theory [46] of the Hall-Petch relation later attributed hardness to the piling up of dislocations at a grain boundary, which concentrates the applied stress to activate dislocation sources in an adjacent grain, thereby propagating slip through the otherwise impenetrable grain boundary. Conrad [47], on the other hand, interpreted the empirical hardness-grain size relation in terms of the relative difficulty of motion of dislocations through the grains, rather than the grain boundaries, and treated smaller grains as more densely populated with dislocations and therefore more impervious to dislocation motion. A further interpretation of the Hall-Petch relation by Li [48] neglected dislocation pile-ups and instead focused on dislocation networks within the grains and considered the grain boundaries themselves to be the dislocation sources. The dependence of the Hall-Petch constant $k_y$ on the grain boundary structure has also been considered [49] in terms of how well grain boundaries are able to sustain stress concentrations. This model suggests that relatively well ordered special grain boundaries with low energy configurations are also rigid and strong; general boundaries, however, are in a more relaxed state and are thus less effective as dislocation barriers.

Recently, a variety of theories based on the microstructure have been proposed to explain whether nanophase materials will harden or soften with grain size refinement into the nanometer regime. Nieh and Wadsworth [50] predicted a critical grain size in this size range at which dislocation pile-ups cannot form, and softening ensues with grain size refinement below this critical size. Aust and coworkers [51] have attributed observed deviations from hardening with decreasing grain size to an increasing number of triple junctions at the smallest grain sizes produced, as suggested previously [52]. Scattergood and Koch [53], using a dislocation network model similar to that of Li [48], have analyzed some existing hardness data for nanophase materials and proposed a critical grain size

below which the dislocation networks are bypassed by moving dislocations, and nanophase material will soften.

3.1.2. *Results.* The results thus far for room temperature microhardness testing of nanophase metals show these materials to be considerably harder than their coarse-grained counterparts. Nanophase Cu, Pd, and Ag [8, 54] with grain sizes between 5 and 60 nm, synthesized by the consolidation of gas-condensed clusters, all demonstrated hardness values ranging from 2 to 5 times those of coarse-grained samples. The hardness of the finest grained nanophase Cu exceeded that attainable from cold-working conventional coarse-grained Cu [54]. The hardness of as-consolidated nanophase Cu and Pd can be increased further with a modest anneal [55].

Hardness improvements appear to be independent of synthesis method: nanophase materials produced by wear [56], inert gas condensation [8, 54, 57], sputtering [58, 59], electrodeposition [60], and mechanical attrition [61, 62] all show similar trends, as shown in Fig. 4. For example, nanophase metals with grains on the order of 10 nm produced by the mechanical attrition of material with grains initially on the order 10 μm hardened by factors ranging from 2 to 7. Nanophase Cu [62] hardened by a factor of 2, while nanophase Ni hardened by factors between 2.5 [62], 6 [51], and 7 [60], and nanophase Fe hardened by factors ranging from about 4 [61] to 5 [62] relative to their coarse-grained antecedents. Intermetallic nanophase TiAl samples with grain sizes of 10-20 nm, produced by sputtering and gas-condensation, hardened by factors from 2 to 4 [59] relative to their coarsed-grained cast precursor target.

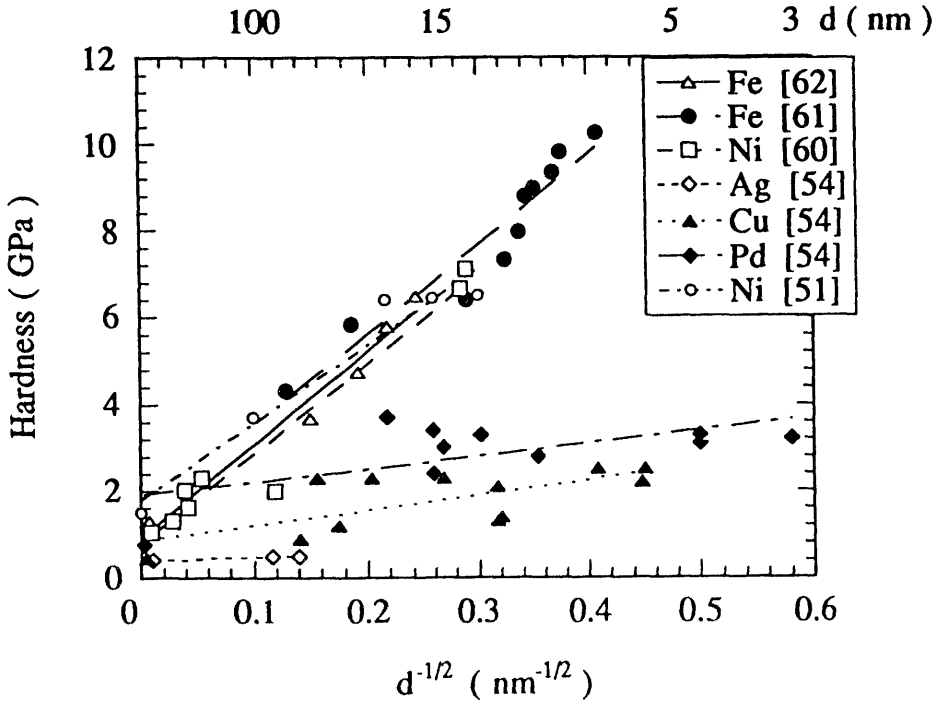


**Figure 4.** Room temperature hardness results versus $d^{-1/2}$, where d is the grain size, for a variety of nanophase metals synthesized from gas-condensed clusters or by mechanical attrition compared with their coarse-grained counterparts (values at $d^{-1/2}$ near zero).

While the hardness typically increases with grain size reduction into the nanometer regime, the results appear to be dependent upon the method used to vary the grain size. Nanophase metals usually exhibit increased hardness with decreasing grain size when individual samples are compared (see Fig. 5a). However, apparently conflicting results indicate that softening of nanophase materials is observed for hardness data derived from samples that have been annealed to increase their grain size (see Fig. 5b). A recent review [67] has compared the results of hardening or softening with the method used to vary the grain size of nanophase metals and intermetallics.

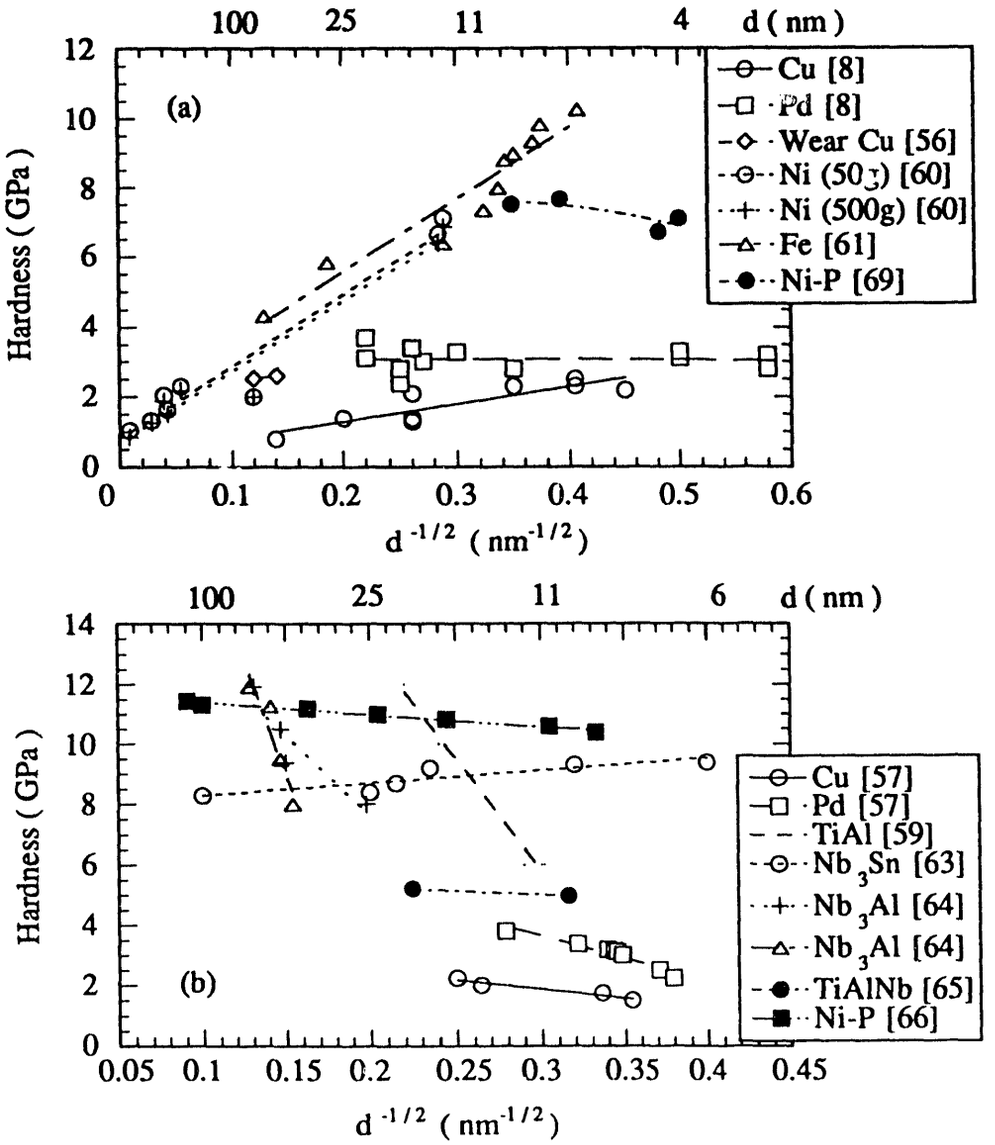


**Figure 5.** Hardness as a function of grain size, showing that the grain size dependence of the hardness is a function of the method used to vary the grain size of the samples: (a) Grain size was changed by using individual samples of different average grain sizes; (b) Grain size was increased by annealing a single sample to grow the grains [67].

Several studies (see Fig. 6) have shown that when individual samples are annealed to grow the grains, initial hardening and subsequent softening can occur. This has been observed in nanophase Cu and Pd [55], TiAl [68], and NiP [69]. Suggestions for the causes of such hardening upon annealing have been porosity reduction [55], changes in the grain boundary structures from nonequilibrium configurations possessing long-range elastic fields [67, 70], and local structural relaxation of the grain boundaries prior to grain growth [36, 71]. The observation of hardening and softening of nanophase TiAl [68] has suggested that two different deformation processes may be dominant over distinct grain size regimes. Thermally activated changes in the structure of the powder particles may be magnified by the large volume fraction of grain boundary phase in nanophase TiAl. Electrodeposited and presumably fully-dense NiP [69] also showed regions of hardening and softening, but these results may have been complicated by phase transformations concurrent with the grain growth during annealing. Thermally treating nanophase samples in the as-produced state may cause changes in the structure of the grain boundaries, densification, phase transformations, and stress relief, any of which may be manifested in the hardness-grain size relation.

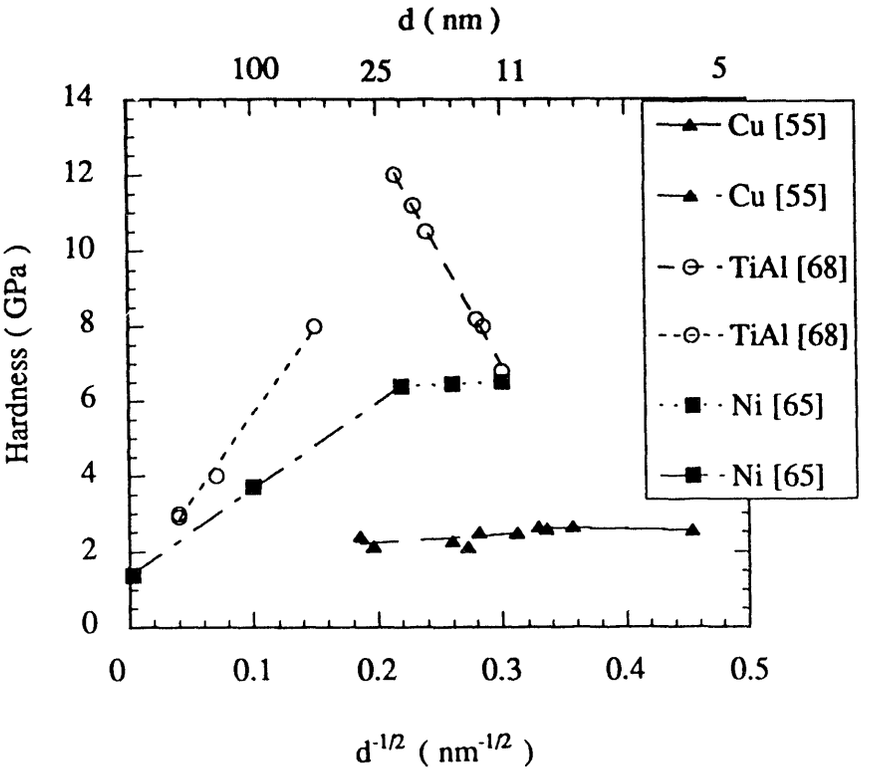


**Figure 6.** Hardness versus grain size. Hardening and softening regimes demonstrated by annealing samples of nanophase Cu [67], TiAl [68] and NiP [69] to grow the grains.

In general, the hardness of metals increases as their grain sizes are reduced into the nanophase regime. However, the extent to which this hardening occurs is not fully clear at this time. The microhardness dependence on the grain size could be lessened in the nanophase grain size regime, as was noted earlier in submicron-grained Ni [72] and seen

in nanophase Pd [54]. This decreased dependence could be related to either the grain boundary structure [49] or to the presence of porosity, flaws, or contamination from synthesis and processing, or to a combination of these effects. At present, it is not clear whether the hardness values measured to date in nanophase materials (mainly metals) are representative of those to be expected in their fully dense and flaw free state, or whether they still represent only lower limits to their ultimate hardness levels.

### 3.2. TENSILE STRENGTH

3.2.1. *Background.* Just as hardness typically derives from the difficulties in creating dislocations and the provision of barriers to dislocation motion, similar mechanisms are responsible for strengthening conventional materials. The challenge to date for nanophase materials has been the acquisition of sufficient volumes of material for tensile strength testing. The testing of a material in uniaxial tension consists of extending a specimen whose longitudinal dimension greatly exceeds the cross-sectional dimensions, all of which need to be large compared with the grain size for reliable measurements to result. The tensile test measures the strength of the material in tension, and typically the data are plotted as stress $\sigma$ (i.e., load per unit cross-sectional area) versus strain $\varepsilon$ (i.e., longitudinal displacement per original or instantaneous longitudinal length).

The information gathered from a tensile test is plotted in such a stress-strain curve with typical regions of elastic deformation, within which nonpermanent stretching of the internal bonds occurs, and a region of plastic deformation, within which dislocations are generated and move through the crystal lattice. The slope of the elastic portion of the stress-strain curve is an indication of the elastic stiffness of the material and is the Young's modulus in a pore-free, flaw-free material. The limit at which the deformation becomes permanent or plastic usually is taken as 0.2% strain, and the stress at which this occurs is the yield strength of the material. The total strain to fracture as well as the stress level at which the sample fails, the fracture stress, are other important parameters that can be obtained from such data. The occurrence of work hardening, in which the material becomes increasingly stronger after yielding because of dislocation interactions, can also be observed. The effects of work hardening can be reduced by the development of necking, in which a localized reduced area in the cross-section causes the stress state to become triaxial; if during necking the material cannot work harden sufficiently to sustain the increasing stress, the localized instability which ensues can cause failure [73].

Enhanced tensile strength of nanophase materials may be expected solely from the difficulty in generation and motion of dislocations [8] in their ultrafine grains that has led to their increased hardness. Changes in elastic moduli can also be expected as materials enter the nanophase regime. Young's modulus is an indication of the elastic stiffness of a material and is determined by the atomic binding forces [3]; however, reduced apparent values of this modulus can result from the presence of sample porosity. Changes in this modulus due to sample porosity have been examined, and the theory developed by Krstic and Erickson [74, 75] for nanophase materials includes a geometrical representation of the pores with sharpened tips [76].

The effects of elevated temperature on the tensile properties of conventional materials are well studied and typically entail reduction in the elastic modulus, reduction in the yield strength, and increased ductility (especially for body-centered cubic materials).

Other deformation processes which are activated by temperature and stress, such as grain boundary sliding, dislocation climb and cross-slip to other slip planes, coupled with changes in the microstructure, such as cavity formation and recrystallization and grain growth, can also change the tensile behavior of conventional materials. It remains to be seen if these changes occur to the same extent in nanophase materials.

3.2.2. *Results.* The nanophase materials tested in tension thus far have been face-centered cubic metals; they have exhibited similar improvements in strength as those seen in their hardness behavior, but they have also showed limited ductility. Relative to their coarse-grained counterparts, the tensile strength of the nanophase metals increased by factors ranging from 1.5 to 8 depending on their grain size and the material [8, 77, 78]. The extent to which the tensile strength improved with grain size refinement to about 25 nm, for example, is on the order of that produced by cold working polycrystalline material [78] (see Fig. 7). The limited levels of ductility exhibited by nanophase metals may possibly arise because of difficulties in creating, multiplying, and moving dislocations, but may as well relate to the presence of significant flaw populations in these materials [8, 79]. Retesting of larger grained (d=50 nm) nanophase Ag did show enhanced ductility and some evidence of work hardening [78] (see Fig. 8). Annealing after consolidation has resulted in improved ductility of cluster consolidated nanophase metals [80] (see Fig. 9) and of mechanically attrited submicron grain-size materials [37].

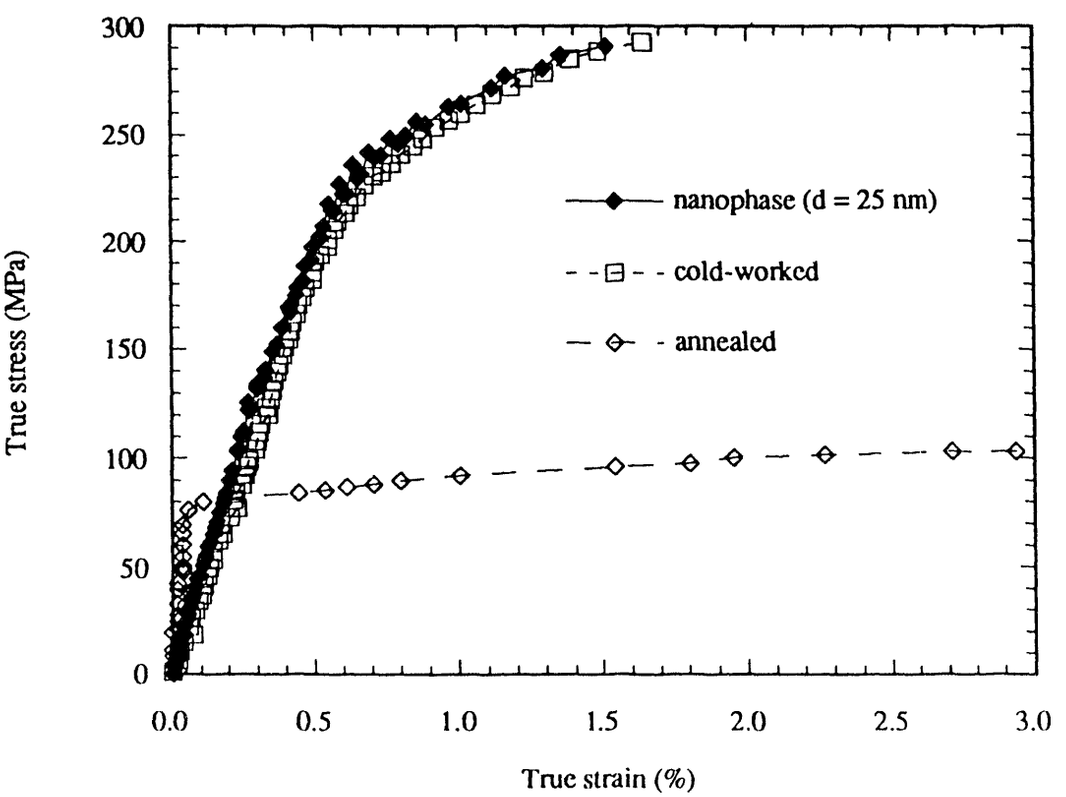


**Figure 7.** Stress-strain curves for samples of nanophase, cold-worked coarse-grained, and annealed coarse-grained copper [78].

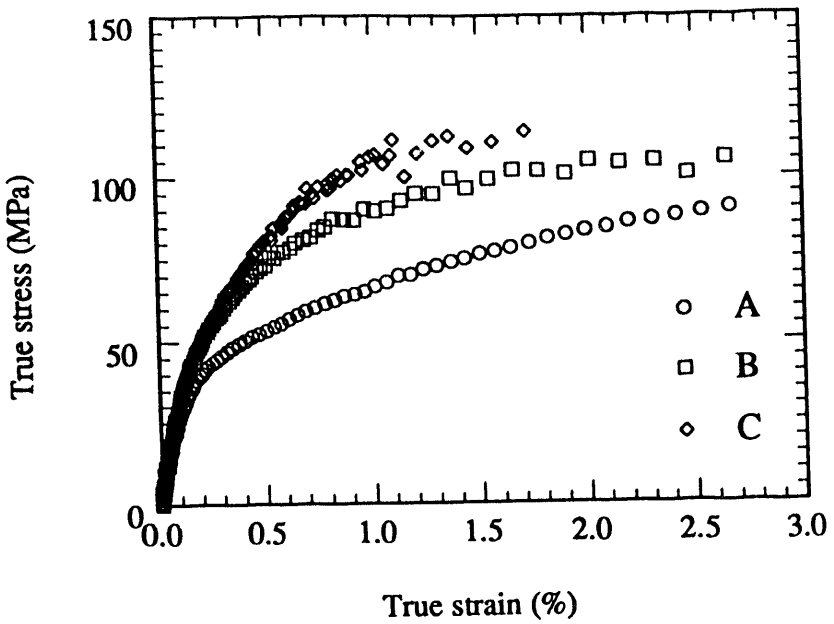


**Figure 8.** Stress-strain curves for a larger grained (d=50 nm) nanophase silver sample, showing evidence of significant ductility and apparent work-hardening in the sample, which was repeatedly tested in the sequence A, B, C [78].

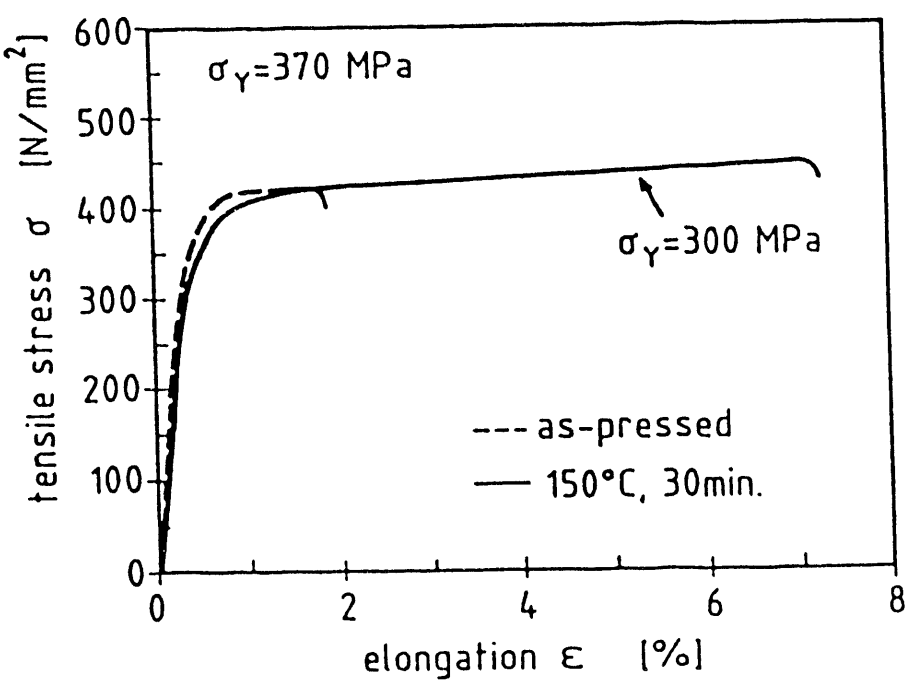


**Figure 9.** Tensile test results for nanophase copper showing increased elongation to failure (microductility), with a small reduction in yield stress from 370 to 300 MPa, when the sample was annealed at a moderate temperature prior to testing [80].

While nanophase metals typically exhibit significant improvements in their tensile strength relative to their coarse-grained counterparts, the true mechanical behavior of nanophase materials may well be camouflaged by the contributions of residual porosity and surface and bulk flaws. For example, the nanophase metals Cu and Pd [78] (see Fig. 10) and Ag [79] were surface polished to improved levels and showed increased tensile strengths. The apparent elastic moduli measured to date on nanophase materials [8, 81] have been decreased in value relative to their coarse-grained counterparts, probably because of porosity. For nanophase Pd samples with residual 4-16% porosities, for example, the apparent Young's modulus values were 2-6 times smaller than that of coarse-grained Pd [8]. This reduction in Young's modulus may be a result of the enhancement of the stress intensity factor from pores in the material. To test this hypothesis, the apparent Young's modulus decrement found in gas-condensed nanophase Pd was contrasted with the Young's modulus of pore-free, electrodeposited, nanophase Ni-P; the fully-dense nanophase Ni-P yielded a Young's modulus value comparable to that for coarse-grained Ni [82]. More recently, the modulus decrement results for nanophase Pd [8] were interpreted in terms of the presence of pores and flaws resulting from processing [77].

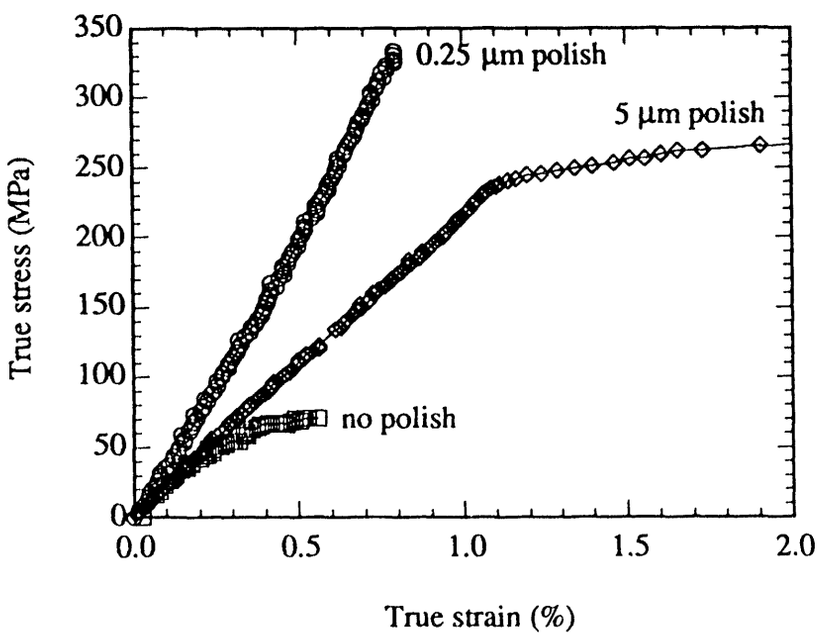


**Figure 10.** Stress-strain curves for nanophase palladium showing that the yield strength of samples polished to ever-finer levels is increased by the removal of surface flaws [8].

### 3.3. COMPRESSIVE STRENGTH, CREEP, AND SUPERPLASTICITY

3.3.1. *Background.* The unique microstructures of nanophase materials are likely to have significant effects on their mechanical behavior. The intercrystalline region composed of grain boundaries and triple junctions can comprise almost 50% of the volume fraction of 5 nm grain size material [83]. This extensive intercrystalline region is expected to have a profound effect on the bulk mechanical behavior, such as ductility and grain boundary

migration and sliding, in nanophase materials. Creep, slow and permanent deformation usually under constant load at an elevated temperature, being primarily controlled by diffusion, is expected to occur readily because of the large volume fraction of uncontaminated grain boundaries and the extant short diffusion distances in nanophase materials. Diffusion along the intergrain contacts is very rapid, and mechanisms similar to those that drive sintering and neck formation, which occur at greatly lowered temperatures for nanophase oxides [84] and at room temperature in nanophase metals, may enhance also the creep rates in these materials. Creep rates may also be influenced by the level of porosity in nanophase samples, since free surfaces tend to increase diffusion rates relative to grain boundary rates [85]. However, creep rates of ceramic powder compacts were shown to be weakly dependent upon porosity as long as it fell below 20% [86].

Brittle materials are better suited for compression strength and creep testing as a more accurate measure of plastic properties because the cracks perpendicular to the applied stress do not propagate [87]. Compression testing of typically brittle ceramics is normally conducted at elevated temperatures (ca. 0.3 to 0.6 $T_m$, where $T_m$ is the absolute melting temperature) in order to take advantage of diffusion-controlled mechanisms that aid the deformation process. The creep rate (measured as the time-dependent change in strain) can be strongly dependent upon the grain size and the temperature through the following constitutive relation for diffusional creep:

$$\frac{d\varepsilon}{dt} = \frac{AD_oGb}{kT}\left(\frac{b}{d}\right)^p\left(\frac{\sigma}{G}\right)^n \exp\left(\frac{-Q}{kT}\right)$$

where A is a numerical constant, $D_o$ is the appropriate diffusivity pre-exponential, G is the shear modulus of the material, k is Boltzmann's constant, b is the magnitude of the Burgers vector, the exponent p defines the grain size dependence, $\sigma$ is the applied stress, n is the stress exponent, and Q is the relevant diffusion activation enthalpy.

For volume or lattice diffusion controlled creep, labeled Nabarro-Herring creep [3], the creep rate is linearly dependent upon the applied stress and dependent on the inverse square of the grain size. For interface diffusion controlled Coble creep [3], the strain rate depends linearly upon the stress (n=1) and diffusion occurs along the grain boundaries resulting in an inverse cube dependence of the creep rate on the grain size (p=3). The Ashby-Verrall model of diffusional creep entails an almost linear dependence of strain rate on the applied stress and typically an inverse $d^3$ behavior [88]. At smaller grain sizes, the Ashby-Verrall creep can be controlled by interfacial reactions involving either grain switching or dislocation motion in which the creep rate has a quadratic dependence on the stress (n=2) and an almost linear dependence on the grain size (p=1) [88]. Thus, the strong dependence of the creep rates on the grain size for these models suggests that grain size refinement from 0.5 μm to 5 nm, for example, would cause a creep rate enhancement by factors ranging from $10^2$ to $10^6$ in nanophase materials.

The basic deformation mechanisms of creep and its associated superplasticity [89] in conventional materials are grain boundary sliding and diffusional processes along the grain boundaries or through the lattice, which can occur solely or in combination. During grain boundary sliding, the strains which develop at the interfaces are usually accommodated by diffusional flow [88], but they can be ameliorated also by dislocation

flow at higher stress and strain rate levels; however, for nanophase materials this latter contribution may be negligible because of limited dislocation activity. The grain switching model of Ashby and Verrall accounts for final retention of grain shape as well as overall dimensional changes in a sample occurring during large scale deformation. In this model, creep deformation involves grain boundary diffusion to achieve intermediate grain shape changes during grain switching and sliding. These intermediate grain shape changes represent an increase in the grain boundary area and require a threshold stress to achieve the associated irreversible work. Therefore, this type of deformation usually occurs at stress levels higher than those required solely for diffusional creep [90]. At elevated temperatures, the primary creep deformation processes are slip, subgrain formation, and grain boundary sliding, and secondary processes include multiple slip, the formation of coarse slip bands and kink bands, and grain boundary migration [3].

Superplasticity is normally considered to be the extreme extensibility of a material, with elongations usually measured between 100 and 5000% in samples with grain sizes or interphase spacings on the order of 1 μm [3]. Superplasticity in conventional materials typically occurs at high temperatures (0.5 $T_m$) and at low strain rates (on the order of $10^{-3}$ $s^{-1}$) [90]. The two parameters indicative of the potential for superplastic deformation are the stress exponent, n, and its reciprocal, the strain-rate sensitivity, m; the higher the value of m, the greater the tensile ductility and the material's resistance to necking. The strain-rate sensitivity is determined by a plot of the logarithm of the stress versus the logarithm of the strain rate. Commonly, in conventional materials, an increase in the strain rate incurs an increase in the flow stress of a material depending upon the material and the temperature [90]. The following simplified empirical equation relates the stress to the strain rate in a material not inclined to work harden:

$$\sigma = K\left(\frac{d\varepsilon}{dt}\right)^m$$

where the constant of proportionality, K, can be a function of the strain rate. The value of m may vary between 0 and 1, the limits for perfectly brittle and perfectly ductile behavior, respectively (the latter value would indicate material that can be drawn to a point without necking). For superplastic metals, m is usually about 0.5, and they exhibit suppressed necking and extensive deformations of 500 to 5000% prior to failure in tension. Conventional ceramics and directionally bonded materials show typical room temperature plasticity on the order of only a few percent; therefore, they are considered superplastic with only 100% strains, and m values for these materials are usually about 0.3.

The microstructures of conventional materials most conducive to the development of superplasticity contain fine (< 10 μm for metals and < 1 μm for ceramics) equiaxed grains [90] that maintain their grain size and shape during deformation; therefore, it is predicted that the ultrafine-grained microstructure of nanophase materials with stabilization against grain growth will make them amenable to high creep rates and large scale deformations that can be used to superplastically form these materials into desired shapes. Conventional superplastic ceramics may contain grain growth inhibitors, such as second phase particles or grain boundary segregants, which suppress static and dynamic grain growth of the ultrafine grains during sintering and deformation [89]. Open porosity has also been credited with stabilization against static and dynamic grain growth of nanophase

ceramics [91]. Another primary concern is adequate grain-boundary cohesive strength, relative to the flow stress, to mitigate cavitation or grain boundary cracking during large strain deformation.

3.3.2. *Results.* Nanophase ceramics have demonstrated greatly enhanced ductility at lower temperatures; in addition, they have been shown recently to exhibit a trend toward superplastic behavior at moderately elevated temperatures based on their measured strain rate sensitivities. The initial indications of plasticity of nanophase ceramics at low temperatures were the hardness results for nanophase $CaF_2$ and $TiO_2$ [92]. The single crystal analogs of these materials failed in a brittle mode; however, when tested at moderate temperatures, the nanophase samples showed plastic deformations of about 100% when compared to their single crystal and polycrystalline coarse-grained analogs. The projection was that nanophase ceramics would be ductile at lower temperatures than those required for coarse-grained ceramics to behave superplastically.

True compressive creep testing of nanophase materials, although limited in the number and variety of materials tested, has substantiated this enhanced plasticity and also increased compressive strength. Compressive creep tests [93] conducted at moderate temperatures on 99% dense nanophase $TiO_2$ showed extensive deformation without crack formation (see Fig. 11); other compressive creep results on nanophase and submicron oxides are limited because the materials were quite porous and during heat treatment, the grains grew dramatically with the disappearance of interconnected porosity after the material achieved 90% of its theoretical density [94, 95]. Similarly, after the mechanical attrition of 75 μm grain size $Fe_{28}Al_2Cr$ powder to produce 80 nm grain size nanophase material, and subsequent shock consolidation, the samples, when tested in compression at room temperature, exhibited extreme plasticity (a true strain of 1.4) and increased yield strength (almost 10 times that of the coarse-grained material) [25].

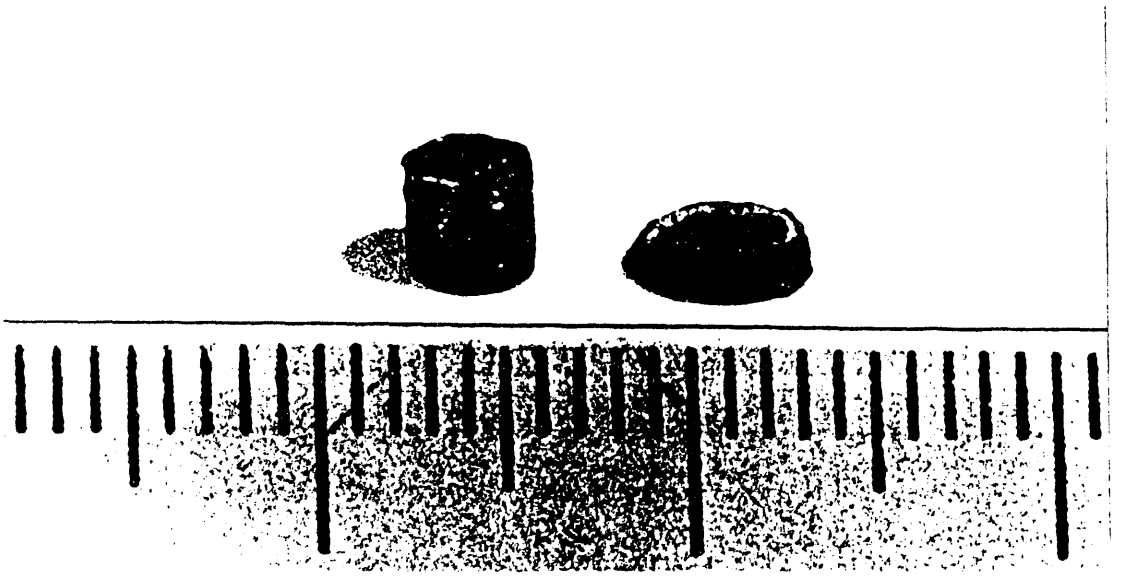

**Figure 11.** Nanophase $TiO_2$ sample before and after compression at 810°C for 15 h [93]. The total strains were as high as 0.6. The small rule divisions are millimeters.

Hardness testing at elevated temperatures can also indicate compressive creep behavior of nanophase materials. Although typically used as a static tool, by increasing the loading times with a constant load and at temperature, the indentation size can be monitored to yield dynamic compressive behavior. In such a way, the indentation sizes on nanophase TiAl were seen to increase in size rapidly and then more slowly, indicating that a diffusion-controlled deformation process was occurring [96]. The data obtained (see Fig. 12) appear to follow the Ashby-Verrall model of creep with a threshold stress occurring above a load of 100 g. At low temperatures, the nanophase TiAl [68] showed little change in hardness until the temperature rose to the point that thermally activated deformation by diffusional creep started. An observed drop in hardness with temperature was attributed partially to densification under the indentation load and primarily to enhanced flow of the material [96].

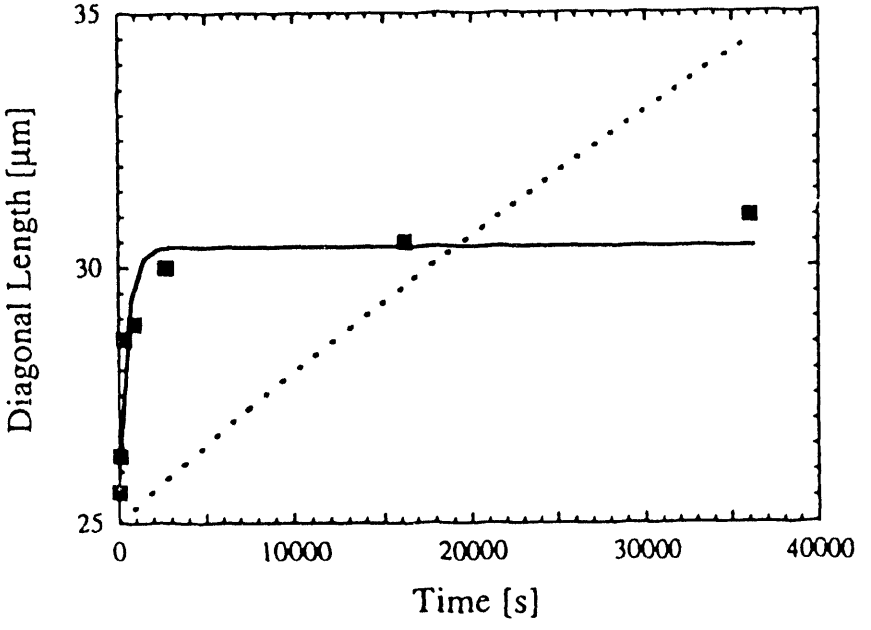


**Figure 12.** Diagonal length of a hardness indent on nanophase TiAl measured at 25°C for a 200g load as a function of time compared with the behavior expected from Coble (·····) or Ashby-Verrall (—) creep [68].

Nanoindentation experiments can show true time dependent behavior of materials under compressive loading as the extent of deformation is measured during both the loading and unloading regimes. Nanophase $TiO_2$ [97] and ZnO [98] measured by nanoindentation experiments at room temperature exhibited the first quantitative results for the strain rate sensitivities. The strain rate sensitivity showed an almost exponential dependence on the grain size in the range of d from about 7 to 50 nm, as shown in Fig. 13. The m values were increased relative to those of coarse-grained ceramics, yet the maximum value (m=0.04) measured at room temperature was still an order of magnitude below that for superplasticity (ca. 0.3). Experimental determinations of the parameters such as m from the creep equation are useful to elucidate the mechanisms governing the deformation of nanophase materials.

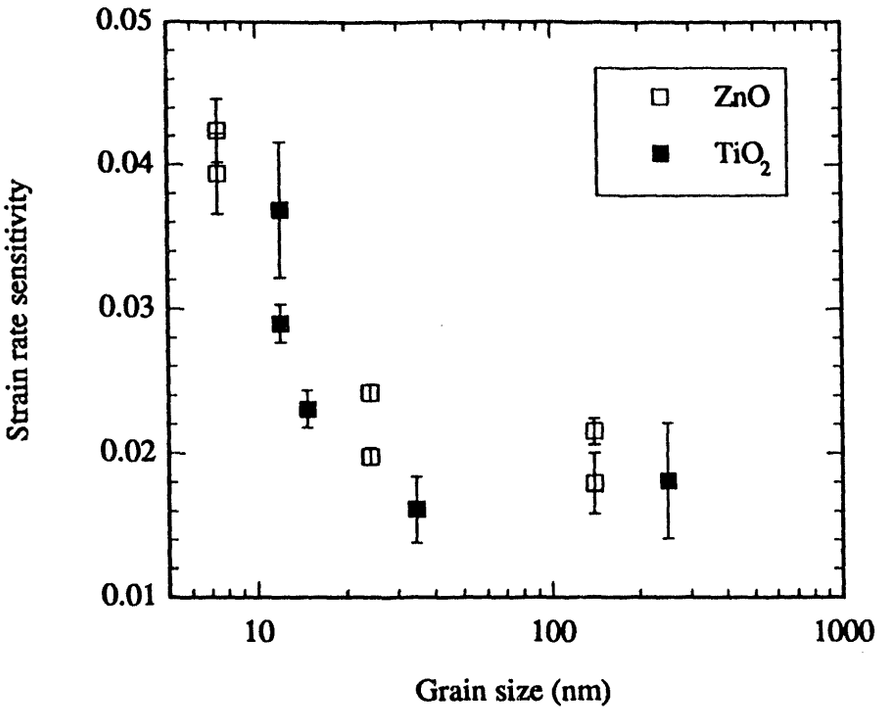


**Figure 13.** Strain rate sensitivity of nanophase $TiO_2$ [97] and ZnO [98] as a function of grain size. The strain rate sensitivity was measured by a nanoindentation method and the grain size was determined by dark-field transmission electron microscopy.

The stress exponent has also been measured in the compressive testing of nanophase ceramics as a method of determining their creep deformation processes. For partially-stabilized zirconia, $ZrO_2$-3 mol% $Y_2O_3$, the measured stress exponent was 3 [99, 100]; the second phase of $Y_2O_3$ added in small quantities can be useful in stabilizing the host material $ZrO_2$ against grain growth as previously discussed. Similar values of n were measured for nanophase $TiO_2$ [93, 101] and $ZrO_2$ [102]; later tests of nanophase $TiO_2$ demonstrated n values between 2.2 and 2.6 [103], very close to the limits of superplasticity. Compressive tests of a nanophase $TiO_2/Y_2O_3$ composite [104] showed $n > 5$. All of these values are much larger than $n = 1$ for the models of diffusional creep; however, a stress exponent of 2 could correspond to interfacial controlled creep [88, 90].

Another indication of the creep mechanisms operating in these materials is the dependence of the strain rate on the grain size. The grain size dependence, p, of the strain rate was measured in nanophase $ZrO_2$-3 mol% $Y_2O_3$ to be 2.66 when the original grain size was used or 4 when the instantaneous grain size was used [105]. The value of p for two studies of nanophase $TiO_2$ was 1.7 in [103] and varied between 1.0 and 1.5 in [104]. However, this parameter may be less meaningful in the quest to determine the phenomena driving creep because the grain size can change dramatically during the course of a high temperature experiment and these changes can be highly dependent in turn on porosity.

Whether nanophase materials can deform superplastically has yet to be determined. If so, these materials could be readily formed to near net shape with great success. Nanophase $TiO_2$ has been formed to a desired shape with excellent detail below 900°C [106]. A test of the formability typically performed on sheet metals [73], the biaxial punch-stretch or bulge test, can be utilized to evaluate the ductility of nanophase materials. Chen and Xue [89] applied this test to ceramics to determine the formability, which like ductility is a function of the flow stress and flaw population. The bulge test is more severe than the typical uniaxial tensile test, since flaws of all orientations can be stressed to cause fracture. Cui and Hahn [107] have recently subjected nanophase $TiO_2$ of 40 nm grain size to bulge tests at temperatures between 700 and 800°C and found ductile behavior. The samples deformed up to true strain levels of 0.1 without the formation of any cracks. These results confirm that the plasticity seen in compressive creep testing also occurs during tensile testing and could be used to form these materials.

Young's modulus values measured on nanophase oxide ceramics have indicated that compression measurements were influenced by the effects of porosity, as was the case for the tensile measurements of metals. Nanoindentation experiments on nanophase $TiO_2$ [97] (initially 75% dense) and ZnO [98] (initially 85% dense) yielded values of the Young's modulus, based on the slope of the loading portion of the indentation curve, between 60 to 80% of that of their fully dense coarse-grained analogs.

The elucidation of the underlying deformation mechanisms of the creep behavior of nanophase materials will be possible when the materials tested are relieved of their residual porosity from processing. Until contributions from densification and from grain growth can be separated from the deformation results, it will be difficult to determine the true creep behavior of nanophase materials in compression. Only then, by using a variety of applied stress and strain rate levels and temperature ranges, can the phenomenological bases for creep be determined for nanophase materials. It will be interesting to determine whether the same mechansims responsible for compressive creep behavior in nanophase materials are those that dominate compressive creep of conventional materials. To date the sole tensile creep measurements on nanophase metals has been for Cu and Pd at low temperatures [8], which showed behavior logarithmic with time and not the accelerated Coble creep suggested by [92].

### 3.4. FRACTURE STRENGTH

3.4.1. *Background.* In the practical application of materials, often it is not the inherent yield strength of the material which limits its application, but its fracture strength. A material can yield and sustain itself against imposed stresses by taking advantage of microstructural features like dislocations and grain boundaries which prolong plasticity. However, a material which has inherently high strength can also fail in a sudden and brittle manner with little plasticity, thereby hindering its usage.

The evolution of fracture of a conventional material occurs in two stages: the nucleation of cracks and their growth to critical crack sizes at which the material cannot sustain the cracks and the material fractures. Nucleation and propagation of cracks can be used to explain the fracture stress dependence on the grain size [108]. Cracks are able to nucleate at inhomogeneities in the microstructure resulting from processing or from deformation (e.g., pores, cavities, dislocation pile-ups). These features concentrate the

applied stress until it reaches the level of the nucleation stress, which bears a $d^{-1/2}$ type relation with the grain size. Reducing the grain size typically either raises the nucleation stress or the stress required to grow the crack and slightly improves the level of ductility in conventional grain-sized materials. Typically, grain size refinement creates a more tortuous path within which the crack must grow and increases the apparent fracture toughness of the material. The area under a stress-strain curve represents the toughness of a material, and tough materials possess high fracture stress levels as well as being ductile with high levels of strain achieved before failure. Fracture toughness is an indication of a material's resistance to fracture and represents the extent to which a material can absorb energy to which it is subjected during testing.

3.4.2. *Results*. The results to date on the fracture properties of nanophase materials have been limited in scope and hindered by the presence of porosity or interfacial phases in the samples tested.

A qualitative study [109] of the fracture surfaces of sintered nanophase $TiO_2$ (d=12 nm) was done to compare these surfaces with those of sintered coarser-grained $TiO_2$ (d=1.3 μm). The lower microhardness and comparable fracture toughness of the coarse-grained material was attributed to the larger and greater number of voids in these samples. A fracture toughness increase in this material of a factor of 2 has also been reported [106]. Predictions of enhanced ductility and fracture toughness also have been offered for nanophase WC-10% Co with 200 nm grain size; the predictions were based on observed hardness increases with grain size refinement [110].

Quantitative estimates of the fracture toughness based on the lengths of cracks emanating from microhardness indentations have been made for nanophase $TiO_2$ [16]. As the grain size of about 10 nm was increased by annealing up to 800°C, the fracture toughness increased by a factor of 3.5 and the hardness increased to the range of well-sintered coarse-grained $TiO_2$. As a result of the sintering, the porosity decreased from 25% to 10% and the grain size increased to about 100 nm; therefore, the contributions of the porosity and of grain size to the mechanical properties cannot be separated as they changed concurrently. Subsequent studies of fully-dense $TiO_2$ indicated that the fracture toughness is independent of the grain size when the grain size is less than 500 nm and is typical of single crystal $TiO_2$ [111].

Bending tests of fully-dense NiP showed that the grain size reduction into the nanometer regime resulted in higher values of the fracture stress and the strain to fracture [112]. The variations in the fracture properties due to grain size were attributed to the changes in the volume fraction and density of the interfaces. However, the acknowledged presence of additional phases of free Ni and $Ni_3P$ complicates the interface-controlled fracture behavior [113].

HREM studies of in-situ fracture of nanocrystalline Au and Au/Si composite films on Al substrates showed a strong dependence of the fracture behavior on the grain size [23]. For grain sizes below 25 nm and slow strain rates, the deformation and fracture were driven by diffusional mechanisms bridging the crack formation and propagation. When the grain size was increased above 35 nm, the cracks grow both through the grains and around the grains. In both grain size regions, the contribution to plasticity by dislocations was deemed negligible because dislocations were not imaged during the testing.

## 4. Conclusions

Most of the research accomplished to date on the mechanical behavior of nanophase materials has dealt with either pure metals or relatively simple oxide ceramics. It may be useful here to summarize the major findings and to make some comparisons between them for these two classes of materials.

The increased strength observed in ultrafine-grained nanophase metals as their grain sizes are reduced into the nanometer regime, although apparently analogous to conventional Hall-Petch strengthening observed with decreasing grain size in coarser-grained metals, must result from fundamentally different mechanisms. An adequate description of the mechanisms responsible for the increased strength observed in nanophase metals will clearly need to accommodate to the ultrafine grain-size scale in these materials and their lack of mobile dislocations. It appears that as this scale is reduced, and dislocation generation and migration become increasingly difficult owing to the confined volumes available in the grains, the energetic hierarchy of microscopic deformation mechanisms or paths is successively accessed. Thus, energetically easier paths (such as dislocation generation from Frank-Read sources) become frozen out at sufficiently small grain sizes and more costly paths become necessary to effect deformation. Just how strong nanophase metals can eventually become will have to be answered after samples are available in which weakening flaws have been removed.

The enhanced strain rate sensitivity observed at room temperature and the evidence of significant plasticity at moderately elevated temperatures found in nanophase ceramics appear to result from increased grain boundary sliding in these materials, aided by the presence of porosity, ultrafine grain size, and probably rapid short-range diffusion as well. The increased strength and limited ductility of nanophase metals, on the other hand, indicates that dislocation generation, as well as dislocation mobility, may become significantly difficult in ultrafine-grained metals. It may thus be that the increased strength of nanophase metals and the increased ductility of nanophase ceramics indicate a convergence of the mechanical response of these two classes of materials as grain sizes enter the nanometer size range. In such a case, grain boundary sliding mechanisms, accompanied by short-range diffusion assisted healing events, would be expected to increasingly dominate the deformation of nanophase materials, and enhanced forming and even superplasticity in a wide range of nanophase materials including metals and alloys, intermetallic compounds, ceramics, and semiconductors could result. As such, increased opportunities for high deformation or superplastic near net shape forming of a very wide range of even conventionally rather brittle and difficult to form materials can be anticipated.

Clearly, much work remains to elucidate the mechanisms responsible for the mechanical behavior of nanophase materials. Critical experiments need to be performed on both metals and ceramics to identify the atomic mechanisms responsible for their observed mechanical properties and a wide range of additional properties need to be measured. Because of the porosity of all nanophase materials synthesized to date, no reliable measurements of the intrinsic elastic properties of these materials exist and their intrinsic plastic deformation behavior has yet to be fully explored. Nevertheless, the very different mechanical behavior already observed for nanophase materials compared with conventional grain size materials indicates that such exploration will be both scientifically interesting and technologically important.

ACKNOWLEDGEMENTS. This work was supported by the U.S. Department of Energy, Basic Energy Sciences - Materials Sciences under Contract W-31-109-Eng-38 at Argonne National Laboratory and Grant DE-FG02-86ER45229 at Northwestern University.

## References

1. M. Nastasi, D. M. Parkin, and H. Gleiter, eds., **Mechanical Properties and Deformation Behavior of Materials Having Ultra-Fine Microstructures** (Kluwer, Dordrecht, 1993).
2. D. Hull and D. J. Bacon, **Introduction to Dislocations**, 3rd ed. (Pergamon, Oxford, 1984).
3. G. E. Dieter, **Mechanical Metallurgy** (McGraw-Hill, New York, 1986).
4. R. W. Siegel, S. Ramasamy, H. Hahn, Z. Li, T. Lu, and R. Gronsky, J. Mater. Res. **3**, 1367 (1988).
5. G. J. Thomas, R. W. Siegel, and J. A. Eastman, Mater. Res. Soc. Symp. Proc. **153**, 13 (1989).
6. G. J. Thomas, R. W. Siegel, and J. A. Eastman, Scripta Metall. et Mater. **24**, 201 (1990).
7. R. Wünderlich, Y. Ishida, and R. Maurer, Scripta. Metall. et Mater. **24**, 403 (1990).
8. G. W. Nieman, J. R. Weertman, and R. W. Siegel, J. Mater. Res. **6**, 1012 (1991).
9. K. Sattler, G. Raina, M. Ge, N. Venkateswaran, J. Xhie, Y. X. Liao, and R. W. Siegel, J. Appl. Phys., to be published (1994).
10. H. E. Schaefer, R. Würschum, M. Scheytt, R. Birringer, and H. Gleiter, Mater. Sci. Forum **15-18**, 955 (1987).
11. H. E. Schaefer, R. Würschum, R. Birringer, and H. Gleiter, Phys. Rev. B **38**, 9545 (1988).
12. H. Hahn, J. Logas, and R. S. Averback, J. Mater. Res. **5**, 609 (1990).
13. W. Wagner, R. S. Averback, H. Hahn, W. Petry, and A. Wiedenmann, J. Mater. Res. **6**, 2193 (1991).
14. P. G. Sanders, J. R. Weertman, J. G. Barker, and R. W. Siegel, Scripta Metall. et Mater. **29**, 91 (1993).
15. D. M. Owen and A. H. Chokshi, Nanostructured Mater. **2**, 181 (1993).
16. R. S. Averback, H. Hahn, H. J. Höfler, J. L. Logas, and T. C. Chen, Mater. Res. Soc. Symp. Proc. **153**, 3 (1989).
17. J. Horvath, R. Birringer, and H. Gleiter, Solid State Commun. **62**, 319 (1987).
18. J. Horvath, Defect and Diffusion Forum **66-69**, 207 (1989).
19. H. Hahn, H. Höfler, and R. S. Averback, Defect and Diffusion Forum **66-69**, 549 (1989).
20. S. Schumacher, R. Birringer, R. Straub, and H. Gleiter, Acta Metall. **37**, 2485 (1989).
21. G. W. Nieman, Ph.D. Dissertation, Northwestern University, Evanston, Illinois (1991) pp. 131-132.
22. P. Gao and H. Gleiter, Acta Metall. **35**, 1571 (1987).

23. W. W. Milligan, S. A. Hackney, M. Ke, and E. C. Aifantis, Nanostructured Mater. 2, 267 (1993).
24. D. G. Morris and M. A. Morris, Acta Metall. et Mater. **39**, 1763 (1991).
25. M. Jain and T. Christman, Acta Metall. et Mater., in press (1993).
26. D. Wolf and J. F. Lutsko, Phys. Rev. Lett. **60**, 1170 (1988); D. Wolf and S. Yip, eds., **Materials Interfaces: Atomic-Level Structure and Properties** (Chapman and Hall, London, 1992).
27. X. Zhu, R. Birringer, U. Herr, and H. Gleiter, Phys. Rev. B **35**, 9085 (1987).
28. U. Herr, J. Jing, R. Birringer, U. Gonser, and H. Gleiter, Appl. Phys. Lett. **50**, 472 (1987).
29. T. Haubold, R. Birringer, B. Lengeler, and H. Gleiter, J. Less-Common Metals **145**, 557 (1988).
30. T. Haubold, R. Birringer, B. Lengeler, and H. Gleiter, Phys. Lett. A **135**, 461 (1989).
31. R. Birringer and H. Gleiter, in **Encyclopedia of Materials Science and Engineering**, Suppl. Vol. 1, R. W. Cahn, ed. (Pergamon, Oxford, 1988) p. 339.
32. R. W. Siegel, in **Materials Interfaces: Atomic-Level Structure and Properties**, D. Wolf and S. Yip, eds. (Chapman and Hall, London, 1992) p. 431.
33. S. K. Ganapathi and D. A. Rigney, Scripta Metall. et Mater. **24**, 1675 (1990).
34. M. L. Trudeau, A. Van Neste, and R. Schultz, Mater. Res. Soc. Symp. Proc. **206**, 487 (1991).
35. B. H. Suits, R. W. Siegel, and Y. X. Liao, Nanostructured Mater., in press (1993).
36. A. Tschöpe and R. Birringer, Acta Metall. et Mater. **41**, 2791 (1993).
37. R. Z. Valiev, N. A. Krasilnikov, and N. K. Tsenev, Mater. Eng. A **137**, 35 (1991).
38. R. W. Siegel and G. J. Thomas, Ultramicroscopy **40**, 376 (1992).
39. R. W. Siegel, Mater. Res. Soc. Symp. Proc. **196**, 59 (1990).
40. N. Rivier, in **Physics and Chemistry of Finite Systems: from Clusters to Crystals**, P. Jena et al., eds. (Kluwer, Dordrecht, 1992) p. 189.
41. R. Cammarata and K. Sieradzki, Phys. Rev. Lett. **62**, 2005 (1989).
42. R. Z. Valiev, in Ref. [1], p. 303.
43. J. Eckert, J. C. Holzer, C. E. Krill, III, and W. L. Johnson, J. Mater. Res. **7**, 1751 (1992); Mater. Res. Soc. Symp. Proc. **238**, 745 (1992).
44. B. H. Suits, M. Meng, R. W. Siegel, and Y. X. Liao, J. Mater. Res., in press (1994).
45. E. O. Hall, Proc. Phys. Soc. London B **64**, 747 (1951); N. J. Petch, J. Iron Steel Inst. **174**, 25 (1953).
46. A. H. Cottrell, Trans. Metall. Soc. AIME **212**, 192 (1958).
47. H. Conrad, Acta Metall. **11**, 75 (1963); in **Ultra-Fine Grain Metals**, J. J. Burke and V. Weiss, eds. (Syracuse University, Syracuse, 1970) p. 213.
48. J. C. M. Li, Trans. Metall. Soc. AIME **227**, 239 (1963).
49. J. W. Wyrzykowksi and M. W. Grabski, Phil. Mag. A **53**, 505 (1986).
50. T. G. Nieh and J. Wadsworth, Scripta Metall. et Mater. **25**, 955 (1991).
51. A. M. El-Sherik, U. Erb, G. Palumbo, and K. T. Aust, Scripta Metall. et Mater. **27**, 1185 (1992).
52. V. B. Rabukhin, Phys. Met. Metalloved **61**, 149 (1986).
53. R. O. Scattergood and C. C. Koch, Scripta Metall. et Mater. **27**, 1195 (1992).

54. G. W. Nieman, J. R. Weertman, and R. W. Siegel, in **Microcomposites and Nanophase Materials,** D. C. Van Aken et al., eds. (TMS, Warrendale, 1991) p. 15.
55. G. E. Fougere, J. R. Weertman, R. W. Siegel, and S. Kim, Scripta Metall. et Mater. **6**, 1879 (1992).
56. S. K. Ganapathi, M. Aindow, H. L. Fraser, and D. A. Rigney, Mater. Res. Soc. Symp. Proc. **206**, 593 (1991).
57. A. H. Chokshi, A. Rosen, J. Karch, and H. Gleiter, Scripta Metall. **23**, 1679 (1989).
58. H. Hahn and R. S. Averback, J. Appl. Phys. **67**, 1113 (1990).
59. H. Chang, H. J. Höfler, C. J. Altstetter, and R. S. Averback, Scripta Metall. et Mater. **25**, 1161 (1991).
60. G. D. Hughes, S. D. Smith, C. S. Pande, H. R. Johnson, and R. W. Armstrong, Scripta Metall. **20**, 93 (1986).
61. J. S. C. Jang and C. C. Koch, Scripta Metall. et Mater. **24**, 1599 (1990).
62. P. Le Brun, E. Gaffet, L. Froyen and L. Delaey, Scripta Metall. et Mater. **26**, 1743 (1992).
63. C. C. Koch and Y. S. Cho, Nanostructured Mater. Lett. **1**, 207 (1992).
64. K. Kim and K. Okasaki, Mater. Sci. Forum **88-90**, 553 (1992).
65. T. Christman and M. Jain, Scripta Metall. et Mater. **25**, 767 (1991).
66. K. Lu, W. D. Wei, and J. T. Wang, Scripta Metall. et Mater. **24**, 2319 (1990 ).
67. G. E. Fougere, J. R. Weertman, and R. W. Siegel, Nanostructured Mater. **3**, in press (1993).
68. H. Chang, C. J. Altstetter, and R. S. Averback, J. Mater. Res. **7**, 2962 (1992).
69. G. Palumbo, U. Erb, and K. T. Aust, Scripta Metall. et Mater. **24**, 2347 (1990).
70. R. Z. Valiev, V. Yu. Gertsman, and O. A. Kabyshev, phys. stat. sol. (a) **97**, 11 (1986).
71. A. L. Greer, in Ref. [1], p. 53.
72. A. W. Thompson, Acta Metall. **23**, 1337 (1975); Acta Metall. **25**, 83 (1977).
73. M. C. Meyers and K. K. Chawla, **Mechanical Metallurgy: Principles and Applications** ( Prentice-Hall, Englewood Cliffs, 1984) p. 583.
74. V. D. Krstic and W. H. Erickson, J. Mater. Sci. **22**, 2881 (1987).
75. V. D. Krstic and W. H. Erickson, J. Mater. Sci. **23**, 4097 (1988).
76. V. D. Krstic, U. Erb, and G. Palumbo, Scripta Metall. et Mater. **29**, 1501 (1993).
77. G. W. Nieman, J. R. Weertman, and R. W. Siegel, Scripta Metall. et Mater. **24**, 145 (1990).
78. G. W. Nieman, J. R. Weertman, and R. W. Siegel, Mat. Res. Soc. Symp Proc. **206**, 581 (1991).
79. A. Kumpmann, B. Günther and H.-D. Kunze, in Ref. [1], p. 312.
80. B. Günther, A. Baalman, and H. Weiss, Mater. Res. Soc. Symp Proc. **195**, 611 (1990).
81. H. Gleiter, Prog. Mater. Sci. **33**, 223 (1989).
82. A. M El-Sherik, U. Erb, V.Krstic, B. Szpunar, M. J. Aus, G. Palumbo, and K. T. Aust, Mater. Res. Soc. Symp Proc. **286**, 173 (1993).
83. K. T. Aust, U. Erb, and G. Palumbo, in Ref. [1], p. 121.
84. R. W. Siegel and H. Hahn, in **Current Trends in the Physics of Materials,** M. Yussouff, ed. (World Scientific, Singapore, 1987) p. 403.
85. R. M. McMeeking and L. T. Kuhn, Acta Metall. et Mater. **40**, 961 (1992).

86. M. N. Rahaman, L. C. De Jonghe, and M.-Y. Chu, J. Amer. Cer. Soc. **74**, 514 (1991).
87. **Metals Handbook**, 9th ed., Vol. 8, Mechanical Testing, (ASM, Metals Park, 1985) p.301.
88. M. F. Ashby and R. A. Verrall, Acta Metall. **21**, 149 (1973).
89. I. W. Chen and L. A. Xue, J. Amer. Cer. Soc. **73**, 2585 (1990).
90. T. A. Courtney, **Mechanical Behavior of Materials** (McGraw-Hill, New York, 1990) pp. 295-309.
91. M.J. Mayo, in Ref. [1], p. 376.
92. J. Karch, R. Birringer, and H. Gleiter, Nature **330**, 556 (1987).
93. H. Hahn, J. C. Logas, H. J. Höfler, and R. S. Averback, Mater. Res. Soc. Symp Proc. **206**, 569 (1991).
94. T. K. Gupta, J. Amer. Cer. Soc. **55**, 276 (1972).
95. M. J. Mayo, D. C. Hague, and D.-J. Chen, Mater. Sci. and Eng. A **166**, 145 (1993).
96. C. J. Altstetter, in Ref. [1], p. 381.
97. M. Mayo, R.W. Siegel, A. Narayanasamy, and W.D. Nix, J. Mater. Res. **5**, 1073 (1990).
98. M. J. Mayo, R. W. Siegel, Y. X. Liao, and W. D. Nix, J. Mater. Res. **7**, 973 (1992).
99. M. Ciftcioglu and M. J. Mayo, Mater. Res. Soc. Symp. Proc. **196**, 77 (1990).
100. M. J . Mayo, in **Superplasticity in Advanced Materials**, S. Hori et al., eds. (Japan Society for Research on Superplasticity, Osaka, 1991) p. 541.
101. H. Hahn and R. S. Averback, J. Amer. Cer. Soc. **74**, 2918 (1991).
102. R. Raj, J. Amer. Cer. Soc. **71**, C-507 (1988).
103. H.-J. Höfler and R. S. Averback, J. Amer. Cer. Soc., submitted (1993).
104. H. Hahn and R. S. Averback, Nanostructured Mater. **1**, 95 (1992).
105. M. J. Mayo, in Ref. [1], p.366.
106. J. Karch and R. Birringer, Ceramics International **16**, 291 (1990).
107. Z. Cui and H. Hahn, Nanostructured Mater. **1**, 419 (1992).
108. P. Nagpal and I. Baker, Scripta Metall. et Mater. **24**, 2381 (1990).
109. Z. Li, S. Ramasamy, H. Hahn, and R. W. Siegel, Mater. Lett. **6**, 195 (1988).
110. L. E. McLandish, B. H. Kear, and B. K. Kim, Nanostructured Mater. **1**, 119 (1992).
111. H. J . Höfler and R. S. Averback, Scripta Metall. et Mater. **24**, 2401 (1990).
112. M. L. Sui, S. Patu, and Y. Z. He, Scripta Metall. et Mater. **25**, 1537 (1991).
113. M. T. Laugier, J. Mater. Sci. Lett. **6**, 841 (1987).

DATE
FILMED
1/31/94
END